Manuscript prepared for J. Name
with version 2014/09/16 7.15 Copernicus papers of the LaTeX class copernicus.cls.
Date: 8 February 2016

An inversion approach for determining distribution of production and temperature sensitivity of soil respiration

Robyn N.C. Latimer[1] and David A. Risk[1]

[1]St. Francis Xavier University, PO Box 5000, Antigonish, Nova Scotia, Canada B2G 2W5

Correspondence to: David Risk (drisk@stfx.ca)

Abstract. Physical soil properties create lags between temperature change and corresponding soil responses, which obscure true Q_{10} values and other biophysical parameters such as depth of production. This study examines an inversion approach for estimating Q_{10} and e-folding depth of CO_2 production (Zp) using physically based soil models, constrained by observed high-frequency surface fluxes and/or concentrations. Our inversion strategy uses a 1-D multi-layered soil model that simulates realistic temperature and gas diffusion. We tested inversion scenarios on synthetic data using a range of constraining parameters, time averaging techniques, mechanisms to improve computational efficiency, and various methods of incorporating real data into the model. Overall, we have found that with carefully constrained data, inversion was possible. While inversions using exclusively surface flux measurements could succeed, constraining the inversion using multiple shallow subsurface CO_2 measurements proved to be most successful. Inversions constrained by these shallow measurements returned Q_{10} and Zp values with average errors of 1.85% and 0.16% respectively. This work is a first step toward building a reliable framework for removing physical effects from high frequency soil CO_2 data. Ultimately, we hope that this process will lead to better estimates of biophysical soil parameters and their variability on short timescales.

1 Introduction

Soil respiration, which includes both root and microbial respiration, represents the largest outward flux of CO_2 from terrestrial ecosystems, with a magnitude far above that of anthropogenic emissions (Raich and Schlesinger, 1992). Small changes in the soil CO_2 flux could therefore have a significant impact on the carbon balance and global atmospheric CO_2 concentrations. In predictions of atmospheric CO_2 over the 21^{st} century, uncertainties surrounding the response of land flux to

climate change are second only to uncertainties surrounding future anthropogenic emissions (Meir et al., 2006). In order to accurately predict future atmospheric CO_2 concentrations, it is crucial to gain a better understanding of how land systems will respond to changing temperature and moisture regimes.

Soil CO_2 production originates from plant root respiration and microbial decomposition of organic matter. The temperature sensitivity of soil respiration describes how the flux of CO_2 from soils will respond to a change in temperature. Normally soil microbial and plant root processes are treated together because they are not readily distinguished from one another. Temperature sensitivity is often quantified by a parameter Q_{10}, which describes the factor increase in soil respiration with a temperature increase of 10^oC. This Q_{10} parameter is used in global climate models to quantify soil feedbacks to climate change. It has been found that Q_{10} values are influenced by a range of environmental factors including soil temperature (Lloyd and Taylor, 1994; Luo et al., 2001), soil volumetric water content (Davidson et al., 1998; Reichstein et al., 2002) and soil organic matter content (Taylor et al., 1989; Wan and Luo, 2003). As these factors exhibit high spatial heterogeneity across ecosystems as well as within a given ecosystem, it has long been expected that Q_{10} will also exhibit high spatial variability. Despite this, most existing models continue to use a globally constant Q_{10} value. This may reduce or enhance predicted release of CO_2 from soils, leading to large over- or under- estimates of the contribution of soil respiration to terrestrial CO_2 flux in the face of climate change. There has been considerable debate over the usage and magnitude of Q_{10} (Davidson et al., 2006; Mahecha et al., 2010), with different studies producing widely variant values. While most studies agree that CO_2 flux feedback will be positive, there is no consensus on how best to estimate the magnitude of Q_{10}.

Historically, Q_{10} values have been determined through regression analysis of soil temperature and CO_2 surface flux measurements. A known source of error in this approach originates in the physics of soil heat and gas transport, which might separate a change in surface soil temperature (normally a 5 cm or 10 cm temperature is used for deriving Q_{10}) from the resultant change in CO_2 flux measured at the surface. The lags depend most heavily on soil heat transport (Phillips et al., 2011), because changes in surface temperature are shifted and dampened significantly as a function of depth, with each successive soil layer experiencing a reduced temperature change in amplitude. Gas diffusion also plays an important role, and even if soil microbes and roots produced CO_2 instantaneously upon receipt of thermal energy at the characteristic production depths, gases still take time to diffuse upward. Soil properties including heat and gas diffusion, and the e-folding depth of CO_2 production (Zp), all contribute to these lags (Fig. 1). Phillips et al. (2011) demonstrated that such lags can lead to severe misinterpretation of data when attempting to extract true Q_{10} values through regression of surface flux and a temperature measurement at a single depth.

These thermal and gas diffusion processes, and the resulting lags, can be captured in a simple 1-D physical heat and gas transport soil model (Nickerson and Risk, 2009; Phillips et al., 2011).

Though not done to date for the soil respiration system, it is possible to use such a model in inverse fashion for estimating the value of parameters like Q_{10} and Zp by looping the forward model iteratively through possible parameter combinations, with observed measurements as a constraint. Normally, an objective function is used for helping decide which parameter set best minimizes the difference between modelled and measured data. This method has been identified as a promising tool for determining unknown soil parameters (Zhou et al., 2009), with an increasing availability of high frequency data sets allowing for rigorous constraints on known model parameters.

This study seeks to develop a reliable inversion framework for determining the Q_{10} and Zp of different sites given continuous soil measurements. It also seeks to provide guidance for researchers who would like to build field observational sites suited for inversion analysis. Working exclusively with synthetic soil data that mimics the form of collected field data and of which all parameters are known, we first undertake sensitivity tests to determine optimal sensor placing in the field, and decide whether soil CO_2 surface flux, and/or profile measurements, are more suited for anchoring inversion approaches with the necessary field data for parameter constraint. Using the best sensor combination, we are able to evaluate the accuracy of the inversion approach in returning the original Q_{10}, and Zp, across many realistic soil type scenarios.

2 Methods

This study uses a one dimensional CO_2 and heat transport model described by Phillips et al. (2011), originally developed by Nickerson and Risk (2009). This model, with existing versions in Perl and R (R Core Team, 2015), was recoded in C to increase computational efficiency for the parameter solving routine.

2.1 Model description

This model (Fig. 2) simulates the movement and production of CO_2 through the soil profile and into the free atmosphere. The model consists of one atmospheric layer and a soil profile 1 m in length, divided into 100 layers of uniform thickness. Each layer can exchange CO_2 with its two nearest neighbouring layers using the 1-D discrete form of Fick's first law:

$$F_{ij} = -D_{ij}\frac{\Delta C_{ij}}{\Delta z_{ij}} \tag{1}$$

where D_{ij} is the effective diffusion coefficient between two soil layers, ΔC_{ij} is the CO_2 concentration difference (μmol m^{-3}) and Δz_{ij} is the difference in depth (m) between the two layers.

For every modelled time step, each soil layer has a defined temperature, biological CO_2 production, CO_2 flux, thermal diffusivity and gas diffusivity. Temperature varies sinusoidally on daily and annual timescales. Changes in surface temperature are shifted and dampened through the soil profile

using:

$$T[i] = T_{avg} + \Delta T_D e^{\frac{-z_i}{d_{Td}}} sin\left(\omega_D t - \frac{-z_i}{d_{Td}}\right) + \Delta T_Y e^{\frac{-z_i}{d_{Ty}}} sin\left(\omega_Y t - \frac{-z_i}{d_{Ty}}\right) \quad (2)$$

$$d_{Td} = \sqrt{\frac{2D_T[i]}{\omega_D}}, d_{Ty} = \sqrt{\frac{2D_T[i]}{\omega_Y}} \quad (3)$$

which simulates the lags related to the rates of thermal diffusion. In this equation, T_{avg} is the average temperature in the air and soil profile for the duration of the simulation, ΔT_D is the amplitude of the daily temperature fluctuation, ΔT_Y is the amplitude of the yearly temperature fluctuation, ω_D is the radial frequency for daily oscillations (ω_D=2π/86400s), ω_Y is the radial frequency for annual oscillations, z_i is the layer depth (m), and D_T is the thermal diffusivity of the soil ($m^2\ s^{-1}$).

Biological CO_2 production in each layer is calculated using an exponentially decreasing function (Nickerson and Risk, 2009):

$$P[i] = \frac{\Gamma_0}{\sum_{i=1}^{N} e^{\frac{-z_i}{Z_p}}} e^{\frac{-z_i}{Z_p}} Q_{10}^{\frac{T[i]-T_{avg}}{10}} \quad (4)$$

where Γ_0 is the total basal soil production (μmol $m^{-3}\ s^{-1}$), N is the number of soil layers, Q_{10} is the temperature sensitivity of soil respiration, z_i is the depth of the layer (m) and Zp is the e-folding depth of CO_2 production (m), defined as the depth below which the total fraction of CO_2 production remaining is 1/e (also called the characteristic production depth in some studies), from which the production at any depth P(i) can be calculated based on equation 4.

Initially, the diffusivity of CO_2 in the soil profile is calculated using the Millington Model (Millingon, 1959), an empirically derived approximation for calculating diffusivity in the field:

$$D_c = \frac{\theta_w^{\frac{10}{3}} \frac{D_{fw}}{H} + \theta_g^{\frac{10}{3}} D_{fg}}{\theta_T^2} \quad (5)$$

D_{fw} and D_{fg} are the diffusivity of CO_2 in free water and free air ($m^2\ s^{-1}$), H is the dimensionless form of Henry's solubility constant for CO_2 in water, and θ_w, θ_g and θ_T are the water filled, air filled and total soil porosities, respectively.

At each time step, the diffusivity of each soil layer is calculated using a temperature correction on this Millington diffusivity:

$$D[i] = D_c \left(\frac{T[i]}{T_{avg}}\right)^{1.75} \quad (6)$$

As previously mentioned, the flux from each layer is determined by Fick's first law, written explicitly as:

$$F[i] = D[i] \frac{(C[i] - C[i-1])}{dz} dt \quad (7)$$

where C[i] is the CO_2 concentration of layer i (μmol m^{-3}), C[i-1] is the concentration of the layer above, and dt is the time step (s).

Finally, at each time step CO_2 concentration in each layer i is calculated using:

$$C[i] = \frac{C_{t-1}\theta_g dz - F[i] + F[i+1] + P[i]}{\theta_g dz} \tag{8}$$

where C_{t-1}[i] is the layer concentration at the previous time step, F[i] is the flux of CO_2 leaving layer i, F[i+1] is the flux of CO_2 entering the layer from the layer below, P[i] is the CO_2 production within layer i.

2.2 Model execution and validation

Before beginning the simulation, the system is initialized using input parameters seen in Table 1. Atmospheric CO_2 concentration remains constant for the duration of the simulation; it is assumed that any flux from the soil will quickly dissipate into the atmosphere. Flux from the bottom soil boundary is set to zero, as production at this depth is negligible according to the exponentially decreasing production function. These system parameters were changed depending on the soil type being simulated.

After initialization, the system undergoes spin-up, during which layer temperatures are held constant at their initial values, and the model is run until the CO_2 concentration in each layer is constant. The duration of the spin up period is dependent on soil diffusivity (and therefore θ_w), and is determined by plotting concentration vs time through the soil profile. This period ranges from 5 to 23 model days within the range of θ_w (0.1 to 0.25). The CO_2 concentration in each layer after spin up is the initial layer concentration at the beginning of the actual simulation.

For each modelled time step (dt=1.0 s), temperature, CO_2 diffusivity, CO_2 production and CO_2 flux are calculated in each soil layer. Every soil layer is then revisited, and the new CO_2 layer concentrations are calculated. The progress of the simulation is monitored by outputting the CO_2 concentration and temperature of specified layers.

2.2.1 Validation

To ensure the model was performing correctly, steady state concentrations through depth (following spin-up) were compared to the steady state solution proposed by Cerling (1984). Daily and yearly temperature fluctuations were removed from the model, and the model was run until CO_2 concentrations in each layer were constant. Deviations of modelled from analytic concentrations were found to be far less than 1%.

2.3 Incorporating constraining data

In this study, we incorporated external data in the same way we would with field studies. We started with real measurements of temperature through depth, and soil volumetric water content, from a local field site. One of the largest challenges in preparing data for inversion is to accurately model soil temperature through depth and time, as temperature is the known determinant of soil lags (Phillips et al., 2011). For each set of temperature measurements through depth, a linear regression (in R) was performed, resulting in a 5th order polynomial for temperature through depth every 1800 s. A linear interpolation through time was performed to obtain temperature values in each layer for every modelled time step. The resultant temperature values replaced our originally sinusoidally varying temperature function in the model. The value of thermal diffusivity was therefore implicitly built into these measurements and is no longer required as a direct model input.

These physical variables were used in a forward instance of the soil model to create CO_2 surface flux and CO_2 concentration timeseries. Datasets were created using many Zp and Q_{10} values of interest, so that we had many idealized datasets on hand in which concentration, fluxes, and associated temperatures, Zp and Q_{10} values, were known. Soil volumetric water content was not formally incorporated as a driver of respiration in these synthetic datasets, so all simulations were performed over periods of constant soil volumetric water content. During inversion we pretended not to know Zp and Q_{10} values of these synthetic datasets, and hoped the inversion process would return the known values. Since the same forward soil model that generated the synthetic datasets was also embedded within the inversion scheme, errors in Zp, or Q_{10}, would be due entirely to the inversion process itself.

2.4 Inversion process

The soil profile CO_2 concentrations and soil CO_2 surface flux are outputs of the simulation. Their values are dependent on all of the system input parameters. A method called inverse parameter estimation is employed to determine the values of Q_{10} and Zp that would have given rise to the observed concentrations and fluxes. Through this process, model outputs are compared to measured field data or synthetic data over a range of model input parameters. The field measurements used in this process will be referred to as the model constraints; these constraints consist of CO_2 concentration measurements at various depths in the soil profile, as well as CO_2 surface flux measurements.

2.4.1 Inversion steps

The model is run for two unknowns, including Q_{10} values ranging from 1 to 5.5 in steps of 0.1, and Zp from 0.02 m to 0.3 m in steps of 0.01 m. This results in a total of 1260 parameter combinations. Inversion seeks to identify the parameter set that minimizes the objective function

$$\sqrt{(S_1 - M_1)^2 + (S_2 - M_2)^2 + (S_3 - M_3)^2 + ...} \tag{9}$$

where S_i and M_i correspond to modelled and measured CO_2 concentrations at various profile depths. For each parameter set, this objective function is calculated every 1800 timesteps and averaged at the end of the simulation. The pair that minimizes Eq. (9) is output as the inversion result.

2.5 Validation of the inverse method

Before applying the inversion method to real field data, tests must be done to ensure method accuracy, and this manuscript focuses on such tests. We created synthetic timeseries using the original soil model, that mimic the form of real data sets. The values of Q_{10} and Zp were known for each synthetic timeseries, as these parameters are required to run the model. This synthetic data included temperature measurements at six depths in the profile, volumetric water content, CO_2 surface flux and CO_2 concentration measurements at various depths in the soil profile.

The inverse method was applied to these synthetic data sets, and the output value of Q_{10} and Zp could then be compared to the actual values of these parameters used to create the timeseries.

2.5.1 Constraint, sensitivity, and random error testing

To determine which model constraints resulted in the highest accuracy of the inversion method, the error (Eq. (9)) was calculated using a large range of constraining parameters and combinations thereof. A total of 35 different constraint combinations were tested, representing various combinations of surface CO_2 flux, and subsurface CO_2 concentration measurements up to 0.6 m depth. These combinations are illustrated in Table 2. Testing which constraints consistently returned the most accurate values of Q_{10} and Zp aids in determining optimal sensor placing the field.

To ensure model validity across all possible parameter values that may be encountered in the field, extensive sensitivity testing was done using these synthetic timeseries. These timeseries were created across a range of combinations of Q_{10}, Zp, volumetric water content (diffusivity) and total soil production. Table 3 illustrates the ranges tested for each parameter.

Field-deployable CO_2 sensors typically have 1-5 % error. To see how the model and inversion would perform under these conditions, errors of 1, 5 and 10 % were added into all components of the synthetic data. The effect of these errors on the inverse method were observed.

3 Results and discussion

Inversions on synthetic timeseries were successful across all tested soil parameters, though some CO_2 concentration measurement depth combinations (surface flux, single or multiple profile measurements) helped to minimize the overall error, as well as the error in Q_{10} and Zp individually. Errors discussed in this section represent an average from 64 inversions across values of Q_{10}, Zp, and soil diffusivity as presented in Table 3. In this section, we use either fractional error ($\frac{|actual-result|}{actual}$), or absolute deviation from the actual value ($|actual - result|$).

3.1 Best measurement configurations to obtain Q_{10} and Zp via inversion

In Fig. 3 we show the average fractional error in the returned Q_{10} value for every combination of subsurface CO_2 sensor measurements. Observations of CO_2 concentration shallow in the soil were found to be necessary for highly accurate Q_{10} estimates. The lowest inversion error for Q_{10} was 1.85%, in a scenario where subsurface measurements were made at 5, 10 and 15 cm. Single concentration measurements at or above 10 cm also proved successful, with errors < 2.3 %. The least accurate inversions for Q_{10} occurred when the constraint consisted of (single or multiple) CO_2 concentration measurements deep in the soil profile. We propose that the poor performance of inversion when using deep profile constraints could be related to the low magnitude of thermal and concentration variability at these depths. Deep soil layers are subject to much smaller thermal fluctuations than layers close to the surface. In this less variable environment, CO_2 concentrations are less variable and provide less of a signal upon which to anchor inversion. In contrast, CO_2 concentrations shallow in the soil exhibited larger variations in temperature and concentration, which presumably allowed Q_{10} to be extracted more easily. If the primary interest is to obtain Q_{10} from inversion, multiple CO_2 concentration measurements in the soil were found to be important. It should be noted that, while differences in error rate were noted, errors for all scenarios could be considered tolerably low relative to the normal variance expected from regression-based Q_{10}, considering the gas transport lags inherent in those data (Phillips et al., 2011).

The average fractional error in Zp for different model sensor combination constraints is also shown in Fig. 3. Out of the 35 combinations tested, only 5 resulted in an average Zp error greater than 2%. Single concentration measurements shallow or deep in the soil profile caused this larger error, but on average, single concentration measurements at any depth in the soil were less accurate. Inversions constrained by at least one measurement shallow ($<$ 15 cm) and one deep ($\geq$ 30 cm) in the profile returned Zp with 100% accuracy across all sensitivity tests. We did expect that single measurements deep in the profile would perform poorly relative to others, because with the exponentially decreasing production defined in the model, CO_2 production approaches zero at significant depths regardless of the value of Zp and thus cannot perform well as an inversion anchor. The large Zp error of almost 25% associated with soil surface CO_2 flux measurements, was also not surprising. In this situation the inversion scheme must reconstruct Zp mainly via the temporal delay, and damping, between sinusoids of temperature through depth, and soil surface CO_2 flux. Without a concentration measurement in the soil, the gas transport regime is black boxed from the perspective of the inversion scheme, resulting in the large error. Overall, surface CO_2 flux measurements alone are less suited for elucidating information on e-folding depth of production, whereas a combination of shallow and deep measurements is best for reconstructing the distribution of CO_2 production in the soil profile.

In examining inversion accuracy for both parameters Q_{10} and Zp simultaneously (Fig. 3), we found that multiple concentration measurements shallow in the soil ($\leq$ 15 cm), or combinations shallow in the soil with one deep concentration measurement ($\geq$ 30 cm) were the best constraints.

Deep soil measurements and surface flux constraints should therefore be avoided if the aim is the minimize overall error. This overall result is a combination of what was found for Q_{10} and Zp individually, where shallow measurements were best for Q_{10} and a combination of shallow and deep measurements resulted in most accurate Zp.

Depending on error tolerance for the final parameter estimates, it is conceivable that the accuracy of all inversions performed here might be sufficient for the community of soil scientists. Out of the 35 combinations tested, 19 resulted in an overall average error less than 5%. The top constraint (measurements at 5,10 and 15 cm) had an average error of 2.01%, and the top 6 combinations all had error less than 3%. These errors are small compared to the degree of random error in CO_2 flux studies (Lavoie et al., 2015). These results are summarized in Table 4, where the top and bottom 5 combinations are listed individually and overall.

This assessment was performed using synthetic data, and even the most ideal field settings will depart from these modelled profiles. For example, we represented CO_2 production through depth using an exponential production function, but a field site may show a linear decrease in production at increasing depths. Clearly users of the inversion process will want to characterize as many site-specific parameters as possible so as to provide proper guideposts and constraints for the inversion, otherwise additional error will be introduced. The sensitivity of the inversion to error is an important question, and will be addressed in a later section.

3.2 Effect of soil-specific parameters on inversion success

Having determined the best CO_2 sensor concentration measurement depth to constrain inversions, we can examine how site-specific parameters such as soil diffusivity, Zp and Q_{10} affect inversion results. For this assessment, we will use the best performing measurement configurations established. Even when not a top choice, we will always include CO_2 surface flux measurements in this section, because of the likelihood that scientists will want to use inversion to analyze these data which are increasing in number rapidly.

Figure 4 a) and b) illustrate how deviation in Q_{10} and Zp were affected by the diffusivity of soils. When subsurface sensor combinations were used as a constraint, there was an overall downward trend in Q_{10} and Zp error with increasing diffusivity. As diffusivity increases (drier soils), CO_2 travels through the soil layers to the surface more quickly which results in decreased lag times, more rapid concentration changes, and more distinct soil responses. Under these conditions of rapid diffusion, inversions were most successful. Sites that are frequently waterlogged with limited air filled pore space tended to be less ideal for inversion, but the optimal instrument configuration still helps ensure reasonably small error throughout the entire range of diffusivities, so there is no strict limitation on the use of the inversion approach in low diffusivity soils.

Figure 4 c) and d) demonstrate the impact of the Zp parameter value on inversion success in terms of deviation in returned Q_{10} and Zp values. For small Zp values, shallow CO_2 concentration

measurements ($\leq$ 15 cm) were the best constraints, presumably because the soil is most active in these top layers. As Zp increases, the production of CO_2 is no longer limited to the shallow soil, the exponential production function decreases more slowly. With increasing Zp, CO_2 production in deeper soil layers is higher, and more useful as an inversion constraint. Some matching of deployment depth was also found, where for example shallow concentration measurements were more accurate for returning the correct value of shallow CO_2 production.

Sensitivity tests indicate that increasing the temperature sensitivity of respiration had opposite effects on Q_{10} and Zp error. Deviation in returned Q_{10} values increased rather uniformly across the best subsurface measurements, while for most subsurface combinations the Zp error decreased. With increasing Q_{10}, respiration becomes more sensitive to temperature changes, leading to larger variations in production in the event of a temperature fluctuation. Figure 4 e) and f) illustrate the impact of this parameter on Q_{10} and Zp error.

With large amounts of existing surface flux data, it is also worth examining the effectiveness of the soil CO_2 surface flux as a constraint, even when it is not the preferred constraint. It is immediately evident from Fig. 4 that inversions constrained by the surface flux resulted in Q_{10} and Zp deviations that responded much differently to changes in soil diffusivity, Zp and Q_{10}. These deviations were often significantly larger than when subsurface constraints were used. Deviations in Q_{10} and Zp generally increased as all three parameters increased. This suggests that for low diffusivity, Zp and Q_{10}, surface flux was a reasonable model constraint, producing errors comparable to the subsurface measurements. This constraint was much less effective for determining depth of CO_2 production. However, Zp was always returned within at least 3.5 cm of its actual value, which for some uses may be an acceptable level of uncertainty. Inversions constrained by surface flux were quite effective in returning Q_{10}. Returning to Fig. 3, the overall average Q_{10} error associated with surface flux was less than 5%, which is significantly better than results using deep subsurface measurements. Figure 4 e) suggests that inversions using large Q_{10} values were responsible for the majority of this error. For Q_{10} of 1.5, these inversions returned Q_{10} with 100% accuracy. For the largest Q_{10}, deviation from the true value climbed as high as 0.6-0.7, which is non-negligible. A shorter model time step could potentially reduce this error, as it may be able to better capture the larger and faster responses associated with high Q_{10} and diffusivity. As we cannot estimate the Q_{10} of a site prior to inversion, however, this insight may not be overly useful in site selection. Overall, inversions constrained by the CO_2 surface flux are possible but should be performed with caution, and with reasonable expectations as to the resultant error level.

It is also of interest to examine how the amount of CO_2 production in the soil profile affects inversion. The bulk of our sensitivity tests were performed using a basal CO_2 production of 10 μmol m^{-3} s^{-1}, which is a fairly high. In order to test the other extreme, several inversions were performed using a production level of 1 μmol m^{-3} s^{-1}. These inversions performed with exactly the same

accuracy as those with a production level of 10. From this, we can conclude that the magnitude of production has no effect on inversion success.

3.2.1 Random error and inversion

The measurements performed by sensors in the field will always be uncertain to some degree. It is therefore important to examine how these uncertainties in recorded temperature, CO_2 and soil volumetric water content measurements will impact the accuracy of the inversion method. Inversions performed on synthetic data to which random errors of 1, 5 and 10% had been added were indeed less accurate than those performed on idealized data. However the resulting errors in returned Q_{10} and Zp were not proportional to the amount of error added to the input data, but actually much lower. That is, errors of 5% in the input data did not result in an additional 5% error in output values. An example of this is illustrated in Fig. 5. This plot demonstrates that with random measurement errors in the ranges of 1-5%, Q_{10} values were still determined with reasonable accuracy. Prior to error addition, deviation in Q_{10} was around 0.12. This deviation increased to 0.14 for 1% error and 0.17 for 5% error. As sensors in the field are typically uncertain by 1 to 5% , the inversion method remains feasible. We can thus conclude that the inversion process is rather tolerant of error in measurement.

3.3 Multi-parameter error landscape

It is worth investigating in detail the error landscape of the inversion process using a multi-parameter sensitivity tests. For this test, we chose the combination of measurements at 5, 10 and 15 cm which had resulted in the most accurate inversions on average.

The results from the sensitivity tests are shown in Fig. 6, panels a) to f). In all combinations, the error in Zp was very small, with the maximum error for any single inversion being just over 2%. Despite this small error, it remains evident which soil conditions should be avoided for most accuracy. Sites with low diffusivity, production deep in the soil and low Q_{10} are the most problematic. This is consistent with the results from Fig. 4 a), c) and e). Trends were not as evident for error in Q_{10}. In panels a), e) and c) the most notable error was found in panel a) for high Zp, low Q_{10}. There is an error in Q_{10} here of almost 15%, which equates to a deviation in Q_{10} of about 0.225 from its actual value. This result is not unreasonable, but it is significantly higher than results from the other inversions. Plot e) demonstrates an interesting result, where there seems to be a valley in the Q_{10} error, illustrating a tradeoff between Zp and diffusivity. This is not evident in the other plots, and does not have an intuitive physical explanation. The effect of Q_{10} on inversion varies, but success hinges quite clearly on soil diffusivity and depth of CO_2 production. Choosing a site in the appropriate ranges of these two parameters will maximize chances of success.

3.4 Limitations and opportunities

There are both limitations and future opportunities for the inversion approach. In general, the better an inversion is constrained with data, the better it will do in returning the true value for parameters of interest. Some of the soil parameters are distributed in ways that must be assumed. For example, the distribution of CO_2 production may be unknown. While most studies in the history of soil modelling have assumed an exponential distribution (and it has been seen in many studies using the gradient technique), some other considerations might help determine whether additional parameterization measurements are needed. For example, knowledge of rooting depth could be one aid. On average, root respiration accounts for 50% of soil respiration (Hanson et al., 2000) and Jackson et al. (1996) provides root distributions for different terrestrial biomes. Jackson et al. (1996) found that tundra, boreal forest and temperate grasslands had upwards of 80-90% of roots within the top 30 cm of soil whereas deserts and temperate coniferous forests had much deeper rooting profiles, with only 50% of roots within the top 30 cm. These and other methods may be helpful in providing constraint data when running inversions on real timeseries.

A future opportunity for inversion studies is to determine depth-specific Q_{10} values, which would be of interest to many researchers. Currently there are few field examples where researchers have determined in-situ Q_{10} as a function of depth, but two examples of such data using include gradient studies include Risk et al. (2008); Tang et al. (2003). Incubations might seem useful in this regard, but are disputed as a representation of in-situ conditions, especially at depth Risk et al. (2008). Ideally, an inversion approach could determine depth-specific Q_{10}, but the reality is challenging. If an additional 100 Q_{10} values were included as unknowns (one for each layer), it would increase computational demand by 100 times. The inversion results would also be confusing, and extreme values at one depth could potentially cause a spurious match to the measured data. The number of non-unique and implausible solutions would rise significantly as a result. A more reasonable approach might be to define Q_{10} as we do Zp, which is as a function of soil depth. This would be computationally compact but whether a function would be realistic is not well known because there are so few examples of Q_{10}-depth profiles against which we could evaluate this approach. The best approach would be to use many profile concentration sensors for constraining data, so that the e-folding depth of production could be known, and the inversion could focus instead solely on determining layer-specific Q_{10} values.

Despite the relatively nascent stage of our soil CO_2 inversion approach, indications are that it has better theoretical validity than traditional regression approaches, which do not take thermal- and gas-transport lags into account. Our error results here compare very favourably against error analyses generated from detailed examination of regression approaches across thermal- and gas-transport parameter space (Zhang et al., 2015; Phillips et al., 2011; Graf et al., 2008).

4 Conclusion

Overall, this inversion method proved successful in testing on synthetic data. Depending on the tolerable level of error for a given application, almost every tested combination resulted in reasonably accurate returned Q_{10} and Zp values. The subsurface concentration measurements that yielded the highest error were typically those that would be of least convenience to install and maintain deep in the soil profile. The other constraint associated with high overall error was CO_2 surface flux, which would likely be the data with highest availability. Most of the error from this constraint arises in estimating the Zp parameter. The CO_2 surface flux is still a reasonable means of estimating Q_{10} values via inversion. While in most cases the error was lower for high diffusivity, shallow production soils, the application of this method is not limited to such regions.

This method is computationally intensive as it performs a sweep through all possible combinations in parameter space. This study used roughly 2.5 core-years of time despite the fact that synthetic timeseries were short. This full sweep ensures that the global minimum in the objective function is located every time, and when solving inversely for two unknown parameters (as we are), this is not an unreasonable approach. However, if it was of interest in the future to examine longer timeseries, or additional parameters such as the depth dependence of Q_{10}, resulting in additional unknown parameters, it may be beneficial to explore other search algorithms to increase efficiency, such as Simulated Annealing.

The next step for this work would be to perform inversions on real timeseries with appropriate measurement constraints, to obtain temperature sensitivity and CO_2 production distribution estimates for various sites. With the increasing availability of high frequency soil data, there would be no shortage in data to analyze. Applying this method for periods of varying constant moisture levels could also help build an understanding of moisture effects on temperature sensitivity of respiration.

Acknowledgements. The authors wish to thank the Natural Sciences and Engineering Research Council (NSERC) and the Atlantic Computational Excellence Network (ACENet) for project resources. We wish also to thank Nick Nickerson and Chance Creelman for valuable comments early on in this research.

References

Cerling, T.E.: The stable isotopic composition of modern soil carbonate and its relationship to climate, Earth Planet. Sci. Lett. 71, 229-240,1984.

Davidson, E.A., Belk, E., Boone, R.D.: Soil water content and temperature as independent or confound factors controlling soil respiration in a temperate mixed hardwood forest, Global Change Biol. 4, 217-227, 1998.

Davidson E.A., Janssens I.A., Luo Y.: On the variability of respiration in terrestrial ecosystems: Moving beyond Q_{10}, Global Change Biol. 12, 154-164, doi: 10.1111/j.1365-2486.2005.01065.x, 2006.

Graf, A., Weihermuller, L., Huisman, J.A., Herbst, M., Bauer, J., Vervecken, H.: Measurement depth effects on the apparent temperature sensitivity of soil respiration in field studies, Biogeosciences, 5, 1175-1188, 2008.

Hanson, P.J., Edwards, N.T., Garten, C.T., Andrews, J.A.: Separating root and soil microbial contributions to soil respiration: A review of methods and observations, Biogeochemistry 48, 115-146, 2000.

Jackson, R.B., Canadell, J., Ehleringer, J.R., Mooney, H.A., Sala, O.E., Schulze, E.D.: A global analysis of root distributions for terrestrial biomes, Oecologia 108, 389-411, 1996.

Lavoie, M., Phillips, C.L., Risk, D.: A practical approach for uncertainty quantification of high-frequency soil respiration using forced diffusion chambers, J. Geophys. Res.: Biogeosciences 120, 128-146, 2015.

Lloyd, J., Taylor, J.A.: On the temperature dependence of soil respiration, Funct. Ecol., 8, 315-323, 1994.

Luo, Y., Wan, S., Hui, D., Wallace, L.L.: Acclimatization of soil respiration to warming in a tall grass prairie, Nature 413, 622-625, 2001.

Mahecha M.D., Reichstein M., Carvalhais N., Lasslop G., Lange H., Seneviratne S.I., Vargas R., Ammann C., Arain M.A., Cescatti A., Janssens I.A., Migliavacca M., Montagnani L., Richardson A.D.: Global Convergence in the Temperature Sensitivity of Respiration at Ecosystem Level, Science 329, 838-840, 2010.

Meir P., Cox P., Grace J.: The influence of terrestrial ecosystems on climate, Trends in Ecol. Evol. 21, 254-260, doi: 10.1016/j.tree.2006.03.005, 2006.

Millington, R.J.: Gas diffusion in porous media, Science 130, 100-102, 1959.

Nickerson, N., Risk, D.: Physical Controls on the Isotopic Composition of Soil Respired and CO_2, J. Geophys. Res.: Biogeosciences 114, G01013, doi: 10.1029/2008JG000766, 2009.

Phillips, C.L., Nickerson, N., Risk, D., Bond, B.J.: Interpreting diel hysteresis between soil respiration and temperature, Global Change Biol. 17, 515-527, doi: 10.1111/j.1365-2486.2010.02250.x, 2011.

R Core Team: R: A language and environment for statistical computing, R Foundation for Statistical Computing, Vienna, Austria. ISBN 3-900051-07-0, http://www.R-project.org, 2015.

Raich J.W., Potter C.S., Bhagawati D.: Interannual variability in global soil respiration, Global Change Biol., 8, 800-812, 2002.

Reichstein, M., Tenhunen, J.D., Roupsard, O., Ourciva,l J.-M., Rambal, S., Dore, S., Valentini, R. Ecosystem respiration in two Mediterranean evergreen Holm oak forests: Drought effects and decomposition dynamics, Funct. Ecol.,16, 27-39, 2002.

Raich, J.W., Schlesinger, W.H.: The global carbon dioxide flux in soil respiration and its relationship to vegetation and climate, Tellus B. 44, 81-99, doi: 10.1034/j.1600-0889.1992.t01-1-00001.x, 1992.

Risk, D., Kellman, L., Beltrami, H., Diochon, A.: In-situ incubations by root exclusion highlight the climatic sensitivity of soil organic matter pools, Env. Res. Lett., 3, 044004, 2008.

Tang, J., Baldocchi, D.D., Qi, Y., Xu, L.: Assessing soil CO_2 efflux using continuous measurements of CO_2 profiles in soils with small solid-state sensors, Ag. For. Met. 118, 207-220, 2003.

Taylor, B.R., Parkinson, D., Parsons, W.F.J.: Nitrogen and lignin content as predictors of litter decay rates: A microcosm test, Ecology, 70, 97-104, 1989.

Wan, S., Luo, Y.: Substrate regulation of soil respiration in a tallgrass prairie: Results of a clipping and shading experiment, Global Biogeochem. Cyc., 17, 1054, doi:10.1029/2002GB001971, 2003.

Zhang, Q., Katul, G.G., Oren, R., Daly, E., Manzoni, S., Yang, D.:The hysteresis response of soil CO_2 concentration and soil respiration to soil temperature. J. Geophys. Res. Biogeosciences 120, 1605-1618, 2015.

Zhou, T., Shi, P., Hui, D., Luo, Y.: Global pattern of temperature sensitivity of soil heterotrophic respiration (Q_{10}) and its implications for carbon-climate feedback, J. Geophys. Res.: Biogeosciences, 114, 9, doi:10.1029/2008JG000850, 2009.

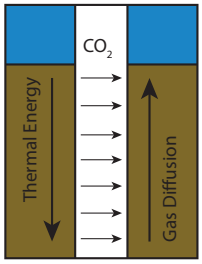

Figure 1. Thermal and gas diffusion lags through a soil profile.

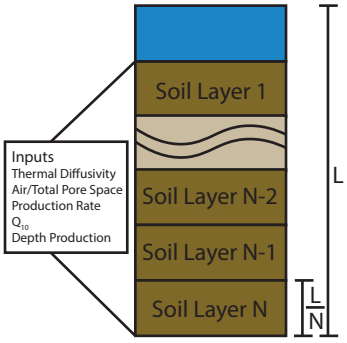

Figure 2. Conceptual representation of the 1-D layered soil model. Overall profile length is denoted with L, and N represents the number of individual layers in the model soil profile.

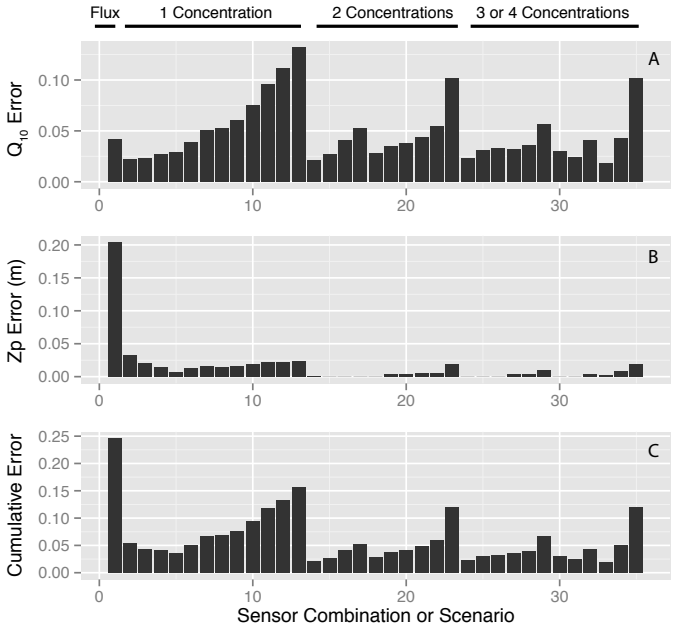

Figure 3. Fractional Error in Q_{10} and Zp individually for different sensor combination scenarios, plus cumulative fractional error in Q_{10} and Zp for the same scenarios.

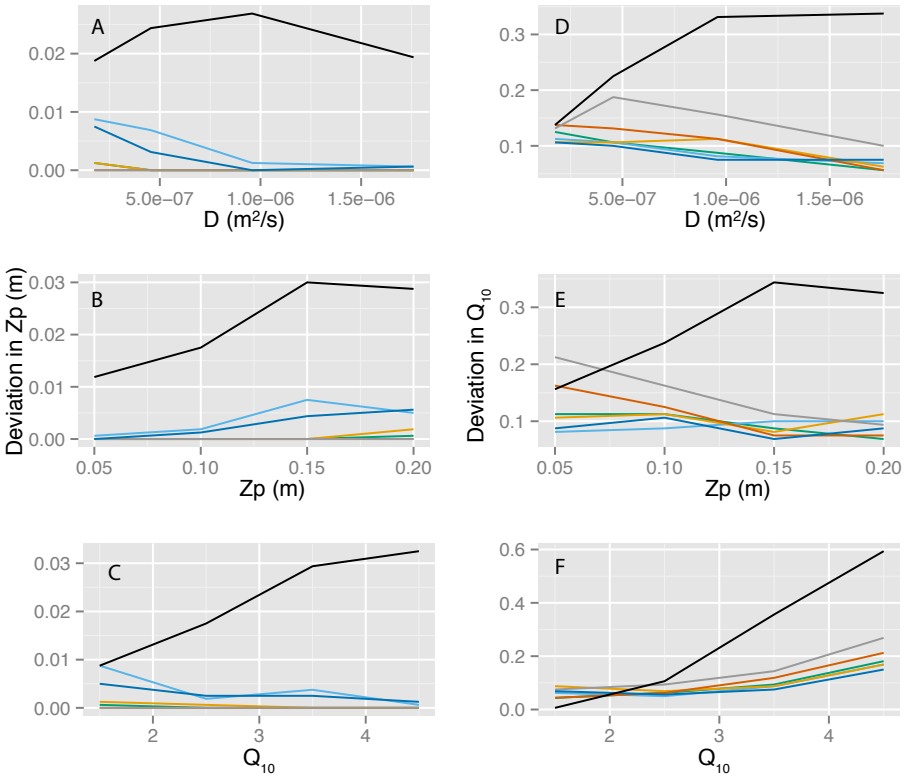

Figure 4. Error in Q_{10} and Zp as a function of Q_{10} (Panels C,F), Zp (Panels B,E) and D (Panels A,D), for a grouping of the best sensor measurement depth combinations. Individual 5 cm and 10 cm observational scenarios are shown in light blue and dark blue, respectively. The 5+15 cm measurement scenario is shown in green. Orange and red illustrate sensitivity of the 5+10+15 cm and 5+10+30 cm scenarios, respectively. Finally, the 4-point 5+15+30+60 cm measurement sensitivity is represented in grey while the surface flux scenario is shown in black. For these sensitivity tests, the known Q_{10} was 2.0, and a Zp of 0.2 m was used.

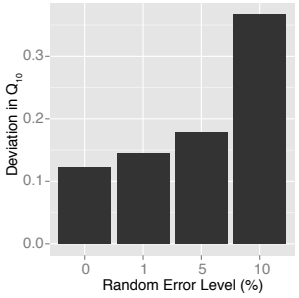

Figure 5. Sample of random error effects on inversion, constrained by one concentration measurement at 5 cm. For this sensitivity test, the known Q_{10} was 2.0.

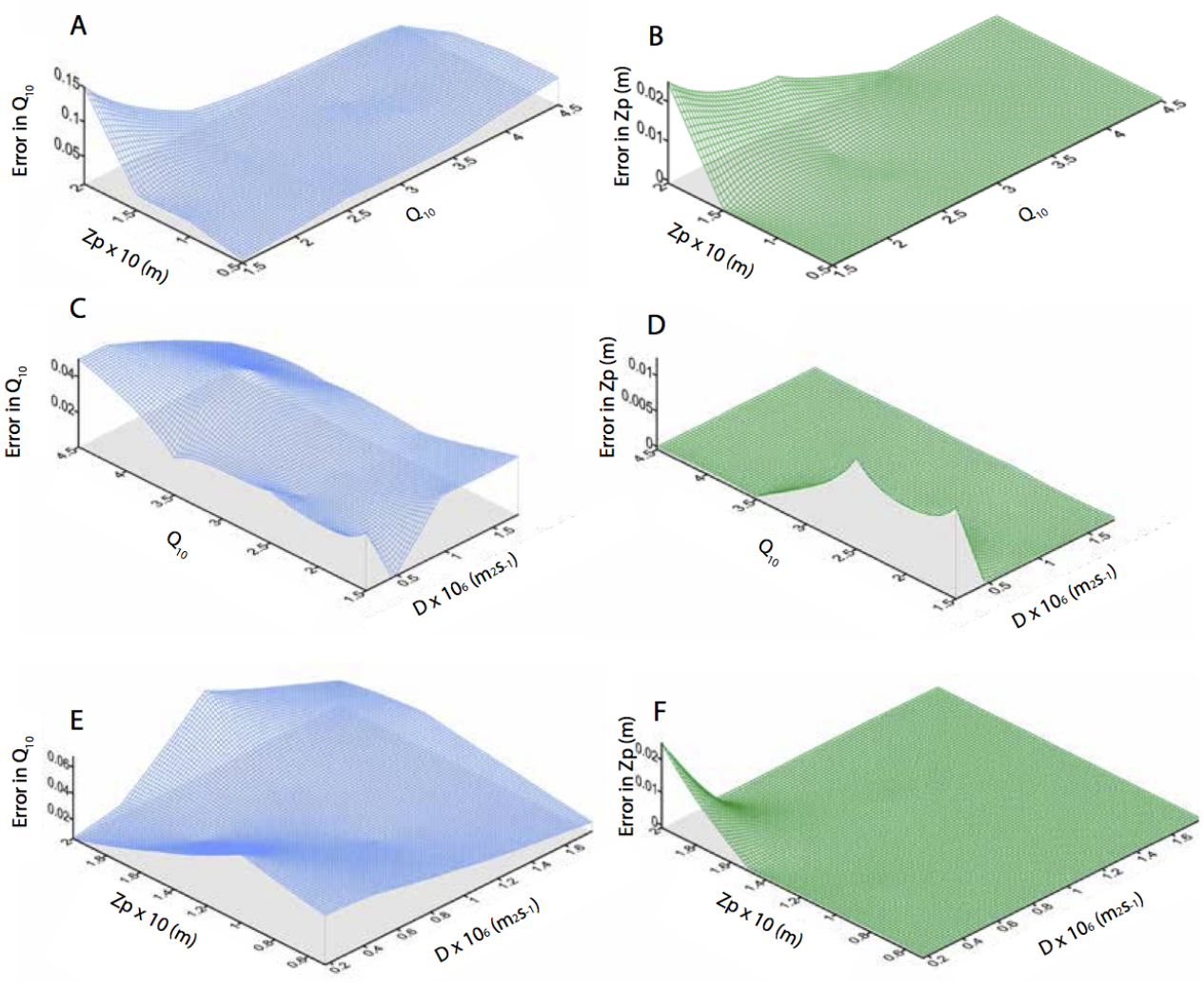

Figure 6. Error in Q_{10} and Zp as a function of Q_{10}, Zp and Diffusivity for the constraint 5+10+15 cm. For these sensitivity tests, the known Q_{10} was 2.0, and a Zp of 0.2 m was used.

Table 1. Default parameter values for simulations

Parameter	Value/Range
Soil porosity (θ_T)	0.40 (v/v)
Thermal diffusivity (D_T)	5 x 10-7 (m^2 s^{-1})
Average air and soil temperature (T_{avg})	15^{o}C
Daily air temperature amplitude (ΔT_D)	5^{o}C
Yearly air temperature amplitude (ΔT_Y)	12^{o}C
Atmospheric CO_2	380 ppm
Total basal CO_2 production (Γ_0)	1 -10 μmol m^{-2} s^{-1}
Production exponential folding depth (Zp)	0.05-0.20 m
Q_{10}	1.5-4.5
Volumetric water content (θ_w)	0.10-0.25 (v/v)

Table 2. Measurement combinations used for the simulations. The combination number is listed at the beginning of each row. The columns represent the type of measurement (e.g. CO_2 surface flux), or the depth of concentration measurement in centimetres. The "X" values denote whether the type or depth of measurement was included in the combination.

Combination	Flux	5	10	15	20	25	30	35	40	45	50	55	60
1	X												
2		X											
3			X										
4				X									
5					X								
6						X							
7							X						
8								X					
9									X				
10										X			
11											X		
12												X	
13													X
14		X		X									
15		X					X						
16		X									X		
17		X											X
18				X			X						
19				X							X		
20				X									X
21							X				X		
22							X						X
23											X		X
24		X		X			X						
25		X		X							X		
26		X		X									X
27				X			X				X		
28				X			X						X
29							X				X		X
30		X		X			X				X		
31		X		X			X						X
32				X			X				X		X
33		X	X	X									
34						X	X	X					
35											X	X	X

Table 3. Default parameter values for sensitivity testing.

Parameter	Abbr.	Minimum	Maximum	Increment
Total basal CO_2 production (μmol m^{-2} s^{-1})	Γ_0	1	10	10
Production exponential folding depth (m)	Zp	0.05	0.2	0.05
Q_{10}		1.5	4.5	1
Volumetric water content (v/v)	θ_w	0.1	0.25	0.05

Table 4. Best and worst sensor combinations for determining Q_{10}, Zp and overall through inversion.

	Combination		
Rank	Q_{10}	Zp	Overall
1	5+10+15 cm	n/a	5+10+15 cm
2	5+15 cm	n/a	5+15 cm
3	5 cm	n/a	5+15+30 cm
4	10 cm	n/a	5+15+30+60 cm
5	5+15+30 cm	n/a	5+30 cm
31	45 cm	55 cm	50 cm
32	50 cm	50 cm	50+60/50+55+60 cm
33	50+60/50+55+60 cm	60 cm	55 cm
34	55 cm	5 cm	60 cm
35	60 cm	Surface Flux	Surface flux